

INDENTATION LOAD/SIZE EFFECT OF STRUCTURAL CERAMIC MATERIALS

**JANA ŠPAKOVÁ, FRANTIŠKA
DORČÁKOVÁ, and JÁN DUSZA**

*Institute of Materials Research SAS, Watsonova 47, 040 01
Košice, Slovakia
jsparkova@imr.saske.sk, fdorcakova@imr.saske.sk,
jdusza@imr.saske.sk*

1. Introduction

Indentation tests like hardness measurement are perhaps the most commonly applied methods for measuring the mechanical properties of materials. The utility of hardness is further enhanced by the fact that it is obtained by a simple test that can be rapidly performed using small samples at moderate cost. However, this utility is partly compromised by the often complex and variable dependence of hardness on several factors such as surface finish, microstructure, indenter load and configuration. Hardness is conventionally determined by applying a load to a material via a geometrically defined indenter, and defined as the ratio of the applied load “P” to the contact area, “A”, of the resultant indent

$$H = \frac{P}{A} = \beta \frac{P}{d^2} \quad (1)$$

where “d” is the characteristic size of resultant indent and “β” is a constant which depends only on the indenter geometry. Two major indenter geometries, Vickers and Knoop, are widely used for hardness testing of structural ceramics. In general, the Vickers hardness “HV” is calculated using the contact area of the indent and the parameter “d” in Eq. (1) is defined as the average of the two diagonals of the square – shaped indent which results in a β-value of 1.8544. In the case of Knoop hardness, the parameter “d” is defined as the length of the long diagonal of the resultant rhombic impression and “β” has a value of 14.229. Moreover investigations have confirmed that the apparent hardness of a given ceramic material is a function of the applied test load, and the measured hardness increases with decreasing test load. To explain this so called “indentation load/size effect – ISE” intensive research has been performed during the last decade and several theories have been occurred for explanation of this. The most common explanation concerns the experimental errors resulting from the limitations of the resolution of the objective lens and the sensitivity of the load cells^{1–3}. According to Bückle² the ISE is directly related to the intrinsic structural factors of the test materials, including indentation elastic recovery, work hardening during indentation, surface dislocation pinning, etc.^{4–6}. It was found that dislocation and twin activities may results in ISE in alumina ceramics with different grain size, too. Another explanation of ISE is the formation of cracks⁷, small ratios of grain size to the indentation size⁸. Conse-

quently, several empirical or semi-empirical equations, including the Mayer’s law^{5,9}, the Hays-Kendall approach¹⁰, the elastic recovery model⁴, the energy-balance approach¹¹, the proportional specimen resistance (PSR) model¹², etc. were proposed for describing the variation of the indentation size with the applied test indentation load. Except of the Mayer’s law, all other approaches involve the determination of a so-called true-hardness, i.e., a load-independent hardness number. It should be mentioned that Hays-Kendall approach frequently gives unrealistic values of load necessary to induce plastic deformation¹², energy-balance approach is essentially a modified form of the empirical Mayer’s law, while the elastic recovery model applies only to plastic materials where slip bands with a particular spacing d_0 between them are produced by indentation. Therefore Hays-Kendall approach and elastic recovery model are not considered here. The most widely used empirical equation for describing the ISE is the Mayer’s law, which gives an expression relating load and size of indentation,

$$P = A \cdot d^n \quad (2)$$

where the exponent “n”, i.e. Mayer’s index, is a measure of the ISE, and “A” is a constant. Parameters “n” and “A” can be derived directly from the curve fitting of the experimental data. When $n < 2$ there is ISE behaviour and when $n = 2$, the hardness is independent of applied load. On the other hand, ISE behaviour may be described by the PSR model¹². In this model, the test – specimen resistance to permanent deformation is assumed not to be a constant, but to increase linearly, and is the directly proportional.

$$W = a_1 d \quad (3)$$

To a first approximation, the form of Eq. (3) can be considered to be similar to the elastic resistance of a spring with the opposite sign to the applied test load. Then, the effective indentation load and the indentation dimension can be related as:

$$P_{\text{eff}} = P_{\text{max}} - W = P_{\text{max}} - a_1 d = a_2 d^2 \quad (4)$$

Eq. (4) means that the proportional specimen resistance (PSR) described by the “ a_1 ”-value and the second coefficient “ a_2 ” can be readily evaluated through the linear regression of “P/d” versus “d”. Thus the applicability of the PSR model to describe the observed ISE in a relatively wider range of applied test load can be examined by testing the linearity between “P/d” and “d”. Eq. (4) can be rearranged as:

$$\frac{P}{d} = a_1 + a_2 \cdot d \quad (5)$$

which enables us to calculate “ a_1 ” and “ a_2 ” from the plots of “ P/d ” against “ d ”. According to the Li and Bradt¹², the parameters “ a_1 ” and “ a_2 ” can be related to the elastic and the plastic properties of the test material, respectively. Especially, a_2 was suggested to be a measure of the so-called true hardness, i.e., load-independent hardness “ H_0 ” ($H_{0(V)}$ -true Vickers hardness, $H_{0(K)}$ -true Knoop hardness)

$$H_{0(V)} = 1,8544 \cdot a_2 \quad H_{0(K)} = 14,229 \cdot a_2 \quad (6)$$

There have been several studies^{13,14} concerning the applicability of the PSR model to describing the ISE of brittle materials.

2. Experimental materials and methods

Three monolithic Al_2O_3 , Si_3N_4 , Si_3N_4 -SiC nanocomposites and ceramic-metal composite WC-Co have been investigated. The monolithic Si_3N_4 was pressure sintered with addition of 3 wt.% Y_2O_3 and 3 wt.% Al_2O_3 by CeramTech (Plochingen, Germany). This monolithic Si_3N_4 is a reference material for European research program ESIS (European Structural Integrity Society) for evaluation of mechanical and physical properties. Pure Al_2O_3 was cold isostatic pressed at 150 MPa and sintered at 1600 °C for 1 h in Faensa (Italy). Si_3N_4 -SiC nanocomposite was prepared by carbothermal reduction from the starting mixture 83.12 wt.% Si_3N_4 , 4.43 wt.% Y_2O_3 , 7.39 wt.% SiO, 4.05 wt.% C in Bratislava (Slovakia). The samples were hot-pressed under a specific heating regime, atmosphere and mechanical pressure at 1750 °C for 2 h. The WC-Co specimens were prepared using standard preparation technique in Šumperk (Czech Republic).

The surface of specimens was ground and polished to 1 μm finish before the mechanical tests. Macrohardness has been measured in a wide range of applied loads from 50 N to 200 N using the testing device HPO 250 for both Vickers and Knoop indenter geometries, and dwell time of 10 seconds. The average values for macrohardness were calculated from 10 measurements. For measuring microhardness by Vickers indenter in load range from 2 N to 10 N a microhardness tester LECO LM 700AT was used. For estimating microhardness by Knoop indenter in the same load range a Zwick/materialprüfung grün Systemtechnik Wetzlar was used and dwell time of 10 seconds. The average values for microhardness were calculated from 20 measurements.

3. Results and discussion

The present data and Mayer’s law

Table I summarizes the Mayer’s law parameters determined by the regression analyses of the results shown in Fig. 1.

The analysis of results listed in Tab. I indicates that, among all test materials, the most significant ISE for Vickers microhardness was observed in Si_3N_4 -SiC nanocomposite ($n = 1.897$) while the ISE in WC-Co (1.922) is negligible. In the case of Knoop microhardness the most significant ISE was observed for Al_2O_3 ($n = 1.746$) while the ISE in Si_3N_4

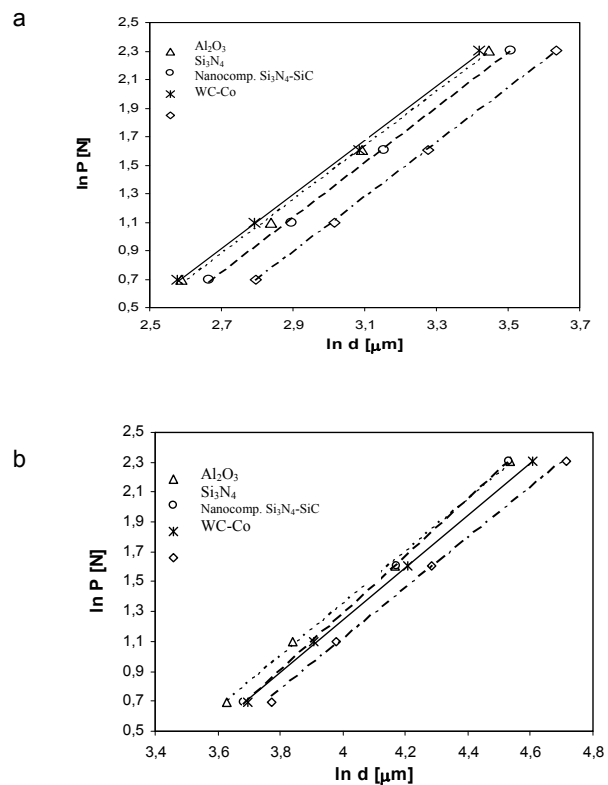


Fig. 1. Dependency of $\ln P$ on $\ln d$ according to the Mayer’s law for tested materials from a) Vickers hardness b) Knoop hardness

Table I

Regression analysis results of the experimental data according to Mayer’s law for Vickers hardness (a) and Knoop hardness (b)

a) Vickers hardness			
Material	n	A	R ²
Si_3N_4	1.922	4.45	0.9994
nanocomp. Si_3N_4 -SiC	1.897	4.21	0.9985
Al_2O_3	1.898	4.25	0.9983
WC-Co	1.922	4.69	0.9999
b) Knoop hardness			
Material	n	A	R ²
Si_3N_4	1.908	6.35	0.9995
nanocomp. Si_3N_4 -SiC	1.749	5.76	0.9996
Al_2O_3	1.746	5.63	0.9986
WC-Co	1.761	5.92	0.9271

($n = 1.908$) is negligible.

It can be seen that the ISE for the Knoop microhardness may be slightly greater than the ISE for the Vickers indentation microhardness. Due to the nature of intrinsic brittleness, Vickers indentation may result in microfracture around the

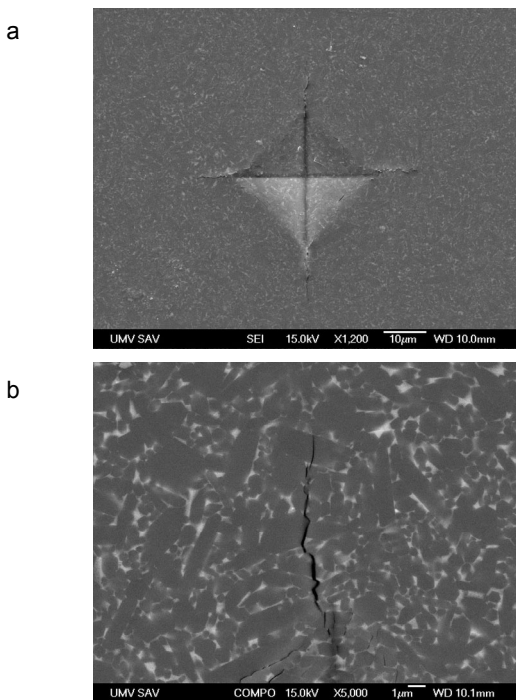


Fig. 2. Formation of indentation radial cracks in Si_3N_4 at 10 N by Vickers indenter (a) detail of indentation radial crack

impression in the surface and/or subsurface of ceramics when the load is high enough¹⁵. Since microfracture occurs mainly during the loading, a portion of energy, which is used to create the indentation deformation will be dissipated by the crack formation shown in Fig. 2.

Thus, one can expect that, for a given material, the hardness value measured with a cracking indentation will be higher than that measured with a crack-free indentation at the same load¹⁶. It seems to be impossible to avoid the effect of microstructure on the hardness measurements in low-load range, in which the ISE is significant, for microcracking can occur in most ceramics even at loads lower than 50 N. On the other hand, when tested below such a low load, the experimental errors related to the small size of the indentation will be significant, sometimes making it impossible to conduct repeatable measurements.

Sargent and Page¹⁷ considered several “n value versus $\ln A$ ” relationships in an attempt to ascertain any possible microstructural effects on those power law parameters. The knowledge of the correlation between “n” and “A” seems to be of little significance for understanding the ISE, because Gong et al.¹⁸ found that the best-fit value of the Mayer’s law coefficient depends on the units system used for recording the experimental data and completely different trends of “n” versus “A” may be observed in different units systems. Previous studies^{19,20} also tried to relate Mayer’s index “n” to the microstructural features. However, knowledge of the generality of the correlation between “n” and grain size is still lacking. In fact, previous studies^{16,21} have pointed out that as pure empirical equation, Mayer’s law cannot provide any knowledge of the origin of ISE.

Proportional specimen resistance “PSR” model

Fig. 3 shows the P/d curves for the tested materials (a—from HV, b—from HK). The best-fit values of the parameters included in Fig. 3 for each material are listed in Tab. II.

Table II
The best-fit results of the PSR model parameters for Vickers hardness (a) and Knoop hardness (b)

a) Vickers hardness				
Material	a_1	a_2	HV ₀ [GPa]	R ²
Si_3N_4	0.0136	0.0086	15.95	0.9986
nanocomp. Si_3N_4 -SiC	0.0182	0.01	18.54	0.9942
Al_2O_3	0.0177	0.0096	17.80	0.9965
WC - Co	0.013	0.0066	12.24	0.9999
b) Knoop hardness				
Material	a_1	a_2	HK ₀ [GPa]	R ²
Si_3N_4	0.0062	0.0011	15.65	0.9991
nanocomp. Si_3N_4 -SiC	0.0186	0.0008	11.38	0.9969
Al_2O_3	0.0187	0.0009	12.81	0.9965
WC - Co	0.0218	0.0006	8.54	0.9823

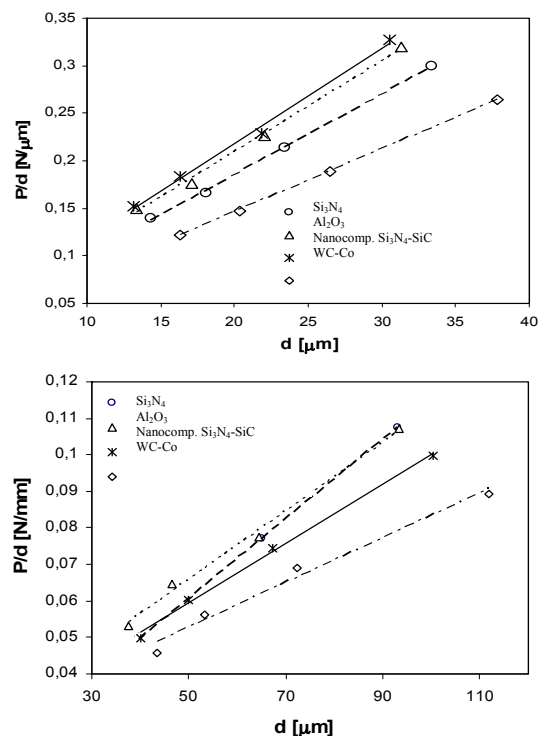


Fig. 3. Dependency of P/d on d according to the PSR model for tested materials from a) Vickers hardness b) Knoop hardness

Dependency of “P/d” on “d” of WC-Co from Knoop hardness reveals nonlinearity. Different behaviour of WC-Co can be explained by the presence of ductile binder phase Co and the significantly lower elastic recovery. The applicability of the PSR model in analyzing the ISE, true hardness was calculated for each material. The results are given in Tab. II, too. As can be seen from Tab. II, it can be concluded, that PSR model may provide a satisfactory explanation for the origin of ISE in microhardness test for various materials. Similar conclusion has been obtained by Li et al.¹². PSR model describes two distinctive regimes of hardness, the indentation load-dependent regime, or ISE regime and the indentation load-independent regime, and Eq. (2) is suggested to be valid in the ISE regime²².

On the other hand, several authors^{21,23} concluded that using the PSR model for ceramics in relatively wide range of applied load can produce several inconsistencies. Experimental results of Gong et al.²⁴ show that at least in some situations, the P/d-d linear relationship can be observed only in a narrow range of applied load. Recently, Sangwal et al.²⁵ and Sahin et al.²⁶ found that behaviour of “P/d” against “d” exhibits two different slopes. The transitions suggests that the phenomenon of the appearance of discontinuities in the conventional P(d) plots for single crystalline samples is connected with the characteristics such as defect structures and grain sizes of the samples. Sangwal et al.²⁷ described that this transition is associated with the processes of relaxation of indentation stresses. Several differences are evident in Tab. II. The slope of the line for the Vickers microhardness is greater than the slope for the Knoop microhardness results. This indicates that the load independent Vickers microhardness for all tested materials is greater than the Knoop values. The values of a_1 are also different. This suggests that ISE for the Vickers microhardness may be greater than that for Knoop microhardness. These results are contrary to the ISE prediction from the n-values of the previous Mayer’s law analysis. Similar conclusion has been obtained by Li et al.²⁸. This is because the Knoop indentation is shallower and has a larger ratio of indentation surface area to the displaced area volume than Vickers indentation. Knoop indentations exhibit much less cracking than Vickers indentation at the same load. Any possible constant hardness threshold due to change in cracking scale may be suppressed until much higher loads, and in any case, any not even be noticeable²⁹. Knoop hardness gradually reaches constant values at very high loads and the Knoop plateau is usually lower than the Vickers plateau values¹⁶. Thibault and Lyinquist³⁰ noted that the onset of serious cracking led to a decrease in the apparent Knoop hardness. This may have been due in part to displacement of the indentation tips or sides, or Swain and Wittling³¹ have recently argued, the crack opening displacement under the Knoop indentation leading to greater indenter penetration. Another reason is that PSR model has been attributed to the elastic properties of the specimens and also to the friction between the indenter facets and the specimen.

4. Conclusions

Independent Knoop and Vickers indentation hardness data of the monolithic Al_2O_3 , Si_3N_4 , Si_3N_4 -SiC nanocomposite

and hardmetal WC-Co have been presented and analyzed by the Mayer’s law and also by application of a proportional specimen resistance (PSR) model. Differences and similarities between the Vickers and Knoop indentation hardness have been observed and discussed.

1. In the test load range, from 2 to 10 N, all the tested materials exhibit a significant indentation load/size effect.
2. Mayer’s law was proved to be sufficient for the description of experimental data. However, no useful knowledge of the origin of the observed ISE may be provided based on this empirical data.
3. The PSR model can be used to analyze the ISE observed in all of tested materials. The PSR model is recommended for determination of load-independent or true hardness.
4. According to PSR model, true Knoop hardness, in comparison with true Vickers hardness exhibits lower value due to cracking. Knoop indentations exhibit much less cracking than Vickers indentation at the same load.

The paper was supported by NANOSMART, Centre of Excellence, SAS, by the Slovak Grant Agency for Science, grant No. 2/7914/2, APVV-0171-06.

REFERENCES

1. Brown A. R. G., Ineson E.: *J. Iron Steel Institute* 169, 376 (1951)
2. Bückle I. H.: *Metall. Rev.* 4, 49 (1959).
3. Mason W., Johnson P. F., Varner J. R.: *J. Mater. Sci.* 26, 6576 (1991).
4. Tarkanian M. L., Neumann J. P., Raymond L., in: *The Science of Hardness Testing and Its Research Applications*, (J. H. Westbrook, H. Conrad, ed.), p. 187. American Society for Metals, Metal Park, OH 1973.
5. Mott B. W.: *Microindentation Hardness Testing*. Butterworths, London 1956.
6. O’Neil H.: *The Hardness of Metals and Its Measurement*. Sherwood, Cleveland 1934.
7. Li H., Bradt R. C.: *J. Mat. Sci.* 31, 1065 (1996).
8. Elmustafa A. A., Eastman J. A., Rittner M. N., Weertman J. R., Stone D. S.: *Scr. Mater.* 43, 951 (2000).
9. Tabor D.: *The Hardness of Metals*. Oxford University Press, Oxford 1951.
10. Hays C., Kendall E. G.: *Metall.* 6, 275 (1973).
11. Quinn J. B., Quin G. D.: *J. Mater. Sci.* 32, 4331 (1997).
12. Li H., Bradt R. C.: *J. Mater. Sci.* 28, 917 (1993).
13. Quinn G. D., Green P., Xu K.: *J. Am. Ceram. Soc.* 86, 441 (2003).
14. Kim H., Kim T.: *J. Europ. Ceram. Soc.* 22, 1437 (2002).
15. Lawn B. R., Wilshaw T. R.: *J. Mater. Sci.* 10, 1049 (1975).
16. Li Z., Ghosh A., Kobayashi A. S., Bradt R. C.: *J. Am. Ceram. Soc.* 72, 904 (1989).
17. Sargent P. M., Page T. F.: *Proc. Brit. Ceram. Soc.* 26, 209 (1978).
18. Gong J. H., Zhao Z., Guan Z. D., Miao H. Z.: *J. Eur. Ceram. Soc.* 2000, 1895.
19. Babini G. N., Bellosi A., Galassi C.: *J. Mater. Sci.* 22, 1687 (1987).
20. Gong J. H., Miao H. Z., Guan Z. D.: *Mater. Sci. Eng., A*

- 303, 179 (2001).
21. Gong J., Wu J., Guan Z.: *J. Eur. Ceram. Soc.* 19, 2625 (1999).
 22. Li H., Han Y. H., Bradt R. C.: *J. Mater. Sci.* 29, 5641 (1994).
 23. Peng Z., Gong J., Miao H.: *J. Eur. Ceram. Soc.* 24, 2193 (2004).
 24. Gong J., Wu J., Guan Z.: *J. Eur. Ceram. Soc.* 19, 2625 (1999).
 25. Sangwal K., Surowska B., Blaziak P.: *Mater. Chem. Phys.* 80, 428 (2003).
 26. Sahin O., Uzun O., Kolemen U., Duzgun B., Ucar N.: *Chin. Phys. Lett.* 22, 3137 (2005).
 27. Sangwal K., Surowska B., Blaziak P.: *Mater. Chem. Phys.* 77, 511 (2003).
 28. Li H., Bradt R. C.: *J. Mater. Sci.* 28, 917 (1993).
 29. Quinn J. B., Quin G. D.: *J. Mater. Sci.* 32, 4331 (1997).
 30. Thibault N. W., Lynquist H. L.: *Trans. ASM* 38, 271 (1947).
 31. Swain M., Wittling M.: *Fracture Mechanics of Ceramics*, 11, (Bradt R. C., Hasselman D. P. H., Munz D., Sakai M., Schevchenko, ed.). Plenum, NY 1996.

J. Špaková, F. Dorčáková, and J. Dusza (*Institute of Materials Research SAS, Watsonova 47, 040 01 Košice, Slovakia*): **Indentation Load/Size Effect of Structural Ceramic Materials**

The Vickers and Knoop hardness of monolithic Al_2O_3 , Si_3N_4 , Si_3N_4 -SiC nanocomposites and a ceramic-metal composite WC-Co in the load range from 2 N to 200 N have been investigated. The experimental results revealed that for each material the Vickers and Knoop hardness in the load range from 2 N to 10 N exhibits a load dependence, i. e. indentation load/size effect (ISE). ISE was analyzed using the Mayer's law and the Proportional Specimen Resistance (PSR) model. Analysis based on Mayer's law can not provide any useful information about the cause of the observed ISE, while true hardness H_0 , which is load independent, can be deduced from the PSR model. According to PSR model, true Knoop hardness, in comparison with true Vickers hardness exhibits lower value due to cracking. The aim of this contribution is to describe indentation load/size effect at Vickers and Knoop hardness test of structural ceramics using the Mayer's law and the Proportional Specimen Resistance (PSR) model.